The Plant Cell, Vol. 26: 4875–4888, December 2014, www.plantcell.org

Stress-Induced Chloroplast Degradation in *Arabidopsis* Is Regulated via a Process Independent of Autophagy and Senescence-Associated Vacuoles[W]

Songhu Wang[a,b] and Eduardo Blumwald[a,1]

[a] Department of Plant Sciences, University of California, Davis, California 95616
[b] Chengdu Institute of Biology, Chinese Academy of Science, Chengdu, Sichuan 610041, China

ORCID ID: 0000-0002-6449-6469 (E.B.)

Two well-known pathways for the degradation of chloroplast proteins are via autophagy and senescence-associated vacuoles. Here, we describe a third pathway that was activated by senescence- and abiotic stress-induced expression of *Arabidopsis thaliana CV* (for chloroplast vesiculation). After targeting to the chloroplast, CV destabilized the chloroplast, inducing the formation of vesicles. CV-containing vesicles carrying stromal proteins, envelope membrane proteins, and thylakoid membrane proteins were released from the chloroplasts and mobilized to the vacuole for proteolysis. Overexpression of *CV* caused chloroplast degradation and premature leaf senescence, whereas silencing *CV* delayed chloroplast turnover and senescence induced by abiotic stress. Transgenic *CV*-silenced plants displayed enhanced tolerance to drought, salinity, and oxidative stress. Immunoprecipitation and bimolecular fluorescence complementation assays demonstrated that CV interacted with photosystem II subunit PsbO1 in vivo through a C-terminal domain that is highly conserved in the plant kingdom. Collectively, our work indicated that CV plays a crucial role in stress-induced chloroplast disruption and mediates a third pathway for chloroplast degradation. From a biotechnological perspective, silencing of CV offers a suitable strategy for the generation of transgenic crops with increased tolerance to abiotic stress.

INTRODUCTION

Environmental stresses such as high salinity, extreme temperatures, and drought are responsible for major losses in yield of major crops worldwide (Mittler and Blumwald, 2010). Plants often use an escape strategy to cope with stress, which is characterized by early flowering and leaf senescence (Levitt, 1972; Ludlow, 1989; Mittler and Blumwald, 2010). During leaf senescence, an early event is the degradation of the chloroplasts, which possess up to 70% of total leaf proteins (Lim et al., 2007; Ishida et al., 2008). The mobile nitrogen resulting from chloroplast disassembly is recycled and supplied to the sink organs, flowers, and seeds (Liu et al., 2008). However, stress-induced chloroplast degradation and premature senescence can affect plant photosynthetic capacity and eventually compromise the crop yield.

Although the inhibition of photosynthetic activity and the degradation of the photosynthetic apparatus are primary targets of abiotic stresses (Rivero et al., 2007), the mechanisms of stress-induced chloroplast degradation remain largely unknown. As an indispensable step of chloroplast degradation, chlorophyll breakdown has been investigated in detail in *Arabidopsis thaliana* (Hörtensteiner, 2009). Five chlorophyll catabolic enzymes that convert green chlorophyll to colorless nonfluorescent chlorophyll catabolites, which are finally degraded in the vacuole, have been identified (Hörtensteiner, 2006, 2009; Sakuraba et al., 2012). Recently, *SGR*, which encodes the nonenzyme protein SGR (for stay-green), has been shown to be a key factor in chlorophyll degradation (Jiang et al., 2007; Park et al., 2007; Ren et al., 2007). In *Arabidopsis*, the SGR protein (NYE1) was able to destabilize the light-harvesting complex II (LHCII) and recruited the five chlorophyll catabolic enzymes to the thylakoids of senescing chloroplast to promote chlorophyll degradation. After chlorophyll degradation, the chlorophyll binding proteins are more susceptible to digestion by chloroplast proteases (Park et al., 2007; Ren et al., 2007; Hörtensteiner, 2009; Sakuraba et al., 2012).

Two pathways have been demonstrated for the degradation of chloroplast stromal proteins: autophagy (Ishida and Yoshimoto, 2008; Ishida et al., 2008; Wada et al., 2009; Izumi et al., 2010) and senescence-associated vacuoles (SAVs) (Otegui et al., 2005; Martínez et al., 2008a; Carrión et al., 2013). Autophagy is a well-known system for the bulk degradation of intracellular proteins and organelles (Ohsumi, 2001; Bassham, 2009). In plants, autophagy has been shown to function in senescence, defense against pathogens, and response to abiotic stress (Bassham, 2009; Reumann et al., 2010; Liu and Bassham, 2012). The chloroplast Rubisco protein and stroma-targeted fluorescent proteins were shown to move to the vacuole via autophagic bodies named Rubisco-containing bodies (RCBs). Dark-induced chloroplast degradation and RCB formation were impaired in autophagy-defective mutants (Ishida and Yoshimoto, 2008; Ishida et al., 2008; Wada et al., 2009). Even whole chloroplasts have been shown to be transported to the vacuole through the autophagy-dependent process in individually

[1] Address correspondence to eblumwald@ucdavis.edu.
The author responsible for distribution of materials integral to the findings presented in this article in accordance with the policy described in the Instructions for Authors (www.plantcell.org) is: Eduardo Blumwald (eblumwald@ucdavis.edu).
[W] Online version contains Web-only data.
www.plantcell.org/cgi/doi/10.1105/tpc.114.133116

darkened leaves (Ishida and Wada, 2009; Wada et al., 2009). Interestingly, RCB-mediated chloroplast degradation was highly activated by carbon rather than nitrogen shortage (Izumi et al., 2010; Izumi and Ishida, 2011). This observation might be partially explained by studies showing that autophagy also participates in chloroplast starch degradation by engulfing small starch granule-like structures from chloroplasts and transporting them to the vacuole for subsequent degradation (Wang et al., 2013).

Senescing leaf cells accumulate an abundance of small SAVs with acidic lumens, and these SAVs can be stained by LysoTracker Red. SAVs have intense proteolytic activity and contain the senescence-associated protease SAG12 (Otegui et al., 2005; Martínez et al., 2008b). Previous studies demonstrated that SAVs contain the chloroplast stromal proteins Rubisco and glutamine synthetase but not the thylakoid proteins D1 and LHCII (Martínez et al., 2008a). Protease inhibitor treatments substantially inhibited Rubisco degradation in detached leaves and completely blocked Rubisco degradation in isolated SAVs (Carrión et al., 2013), suggesting that SAVs are a lytic compartment for degradation rather than a shuttle compartment for carrying chloroplast proteins to the central vacuole (Martínez et al., 2008b).

In spite of the increasing information regarding processes associated with the degradation of chloroplast stroma proteins, the pathway(s) by which thylakoid membrane proteins are released from the chloroplast and transported to the vacuole for degradation remain poorly understood. Here, we identified a nucleus-encoded gene, *CV* (for chloroplast vesiculation), that targets and destabilizes chloroplasts for protein degradation and induces the formation of vesicles containing thylakoid proteins. The CV-containing vesicles (CCVs) are released from the chloroplasts and mobilized to the vacuole for degradation through a pathway that is independent of autophagy and SAVs.

RESULTS

CV Expression Was Activated by Abiotic Stress and Senescence but Suppressed by Cytokinin

During abiotic stress, the breakdown of the plant photosynthetic machinery is a major factor in the reduction of CO_2 assimilation by stressed plants (Tambussi et al., 2000). It has been shown previously that the cytokinin-dependent inhibition of drought-induced senescence resulted in sustained photosynthetic activity during the stress episode and that it enhanced tolerance to water deficit (Rivero et al., 2007, 2009, 2010). The expression of isopentenyl synthase (IPT), encoding a key enzyme in cytokinin synthesis, under the control of a maturation- and stress-induced promoter (pSARK) leads to the protection of the photosynthetic apparatus and enhanced chloroplast stability (Rivero et al., 2010; Reguera et al., 2013). Using DNA microarrays, we analyzed RNA expression patterns in wild-type and transgenic pSARK-IPT rice (*Oryza sativa*) plants during water deficit (Peleg et al., 2011; Reguera et al., 2013). The expression of one gene encoding a chloroplast protein with unknown function (LOC_Os05g49940) was activated by stress in the wild-type plants but not in the transgenic pSARK-IPT plants (Peleg et al., 2011).

The *Arabidopsis* genome contains At2g25625, a gene homolog to LOC_Os05g49940, whose function remains to be characterized. The public microarray database (Winter et al., 2007) indicated that although At2g25625 expression was barely detectable in young tissues, its expression was greatly induced by abiotic stress and senescence during extensive chloroplast degradation (Hörtensteiner, 2006; Martínez et al., 2008b). Therefore, we surmised that the gene could play a role(s) in chloroplast destabilization.

The gene in *Arabidopsis* (At2G25625) was cloned and named *CV* due to the subcellular localization of the encoded protein and its functions as revealed in this study. As indicated by quantitative RT-PCR assays (Figures 1A and 1B), *CV* expression was activated by senescence and abiotic stresses such as salt stress and methyl viologen (MV)-induced oxidative stress. *CV* expression was significantly downregulated by a 3-h treatment with cytokinin (Figure 1C), a phytohormone that delays senescence (Gan and Amasino, 1995). To study the tissue-specific expression of *CV*, we cloned its native promoter, a 2-kb region upstream of the start codon, and used it to drive the reporter gene β-glucuronidase (*GUS*). The GUS staining assays of transgenic ProCV-GUS plants suggested that *CV* was expressed strongly in senescent and mature leaves but not in young leaves of 40-d-old plants (Figure 1D). In leaves from 21-d-old seedlings, *CV* expression was barely detectable, but its expression was substantially enhanced by salt stress treatment (Figure 1E).

CV Targets Chloroplasts and Induces Vesicle Formation in Chloroplasts

CV is predicted to contain a chloroplast transit signal peptide at the N terminus using the ChloroP 1.1 server (http://www.cbs.dtu.dk/services/ChloroP/). In order to assess CV subcellular localization, we fused the enhanced green fluorescent protein (GFP) to the C terminus of CV. The fusion gene *CV-GFP* was transiently expressed in cotyledons of *Arabidopsis* plants constitutively expressing stroma-targeted DsRed (CT-DsRed) (Ishida et al., 2008). Confocal microscopy observations indicated that CV-GFP became localized in chloroplasts and was concentrated in some vesicle-like spots (Figure 2A). The CCVs also aggregated outside of the chloroplast in some unknown compartments that included the stroma-targeted DsRed but not chlorophyll (Supplemental Figure 1A). Interestingly, CV-GFP localized in both the cytosol and chloroplasts in epidermal cells (Supplemental Figure 1B). Expression of GFP alone resulted in a green fluorescence signal not associated with chloroplasts (Figure 2B). In addition, the movement of CCVs departing from chloroplasts was captured by time-lapse observation via confocal microscopy (Supplemental Figure 1C).

The chloroplast localization of CV was further assessed by immunolabeling using antibodies raised against GFP (Figures 2C to 2E). The immunolabeled gold particles were mostly associated with thylakoids or envelope membranes rather than stroma before the formation of vesicles (Figure 2C). The membrane association of CV can be explained by its predicted transmembrane domain (http://aramemnon.botanik.uni-koeln.de/) (Supplemental Figure 2). In some CV-labeled chloroplasts, the envelope membrane lost integrity (Supplemental Figure 3A)

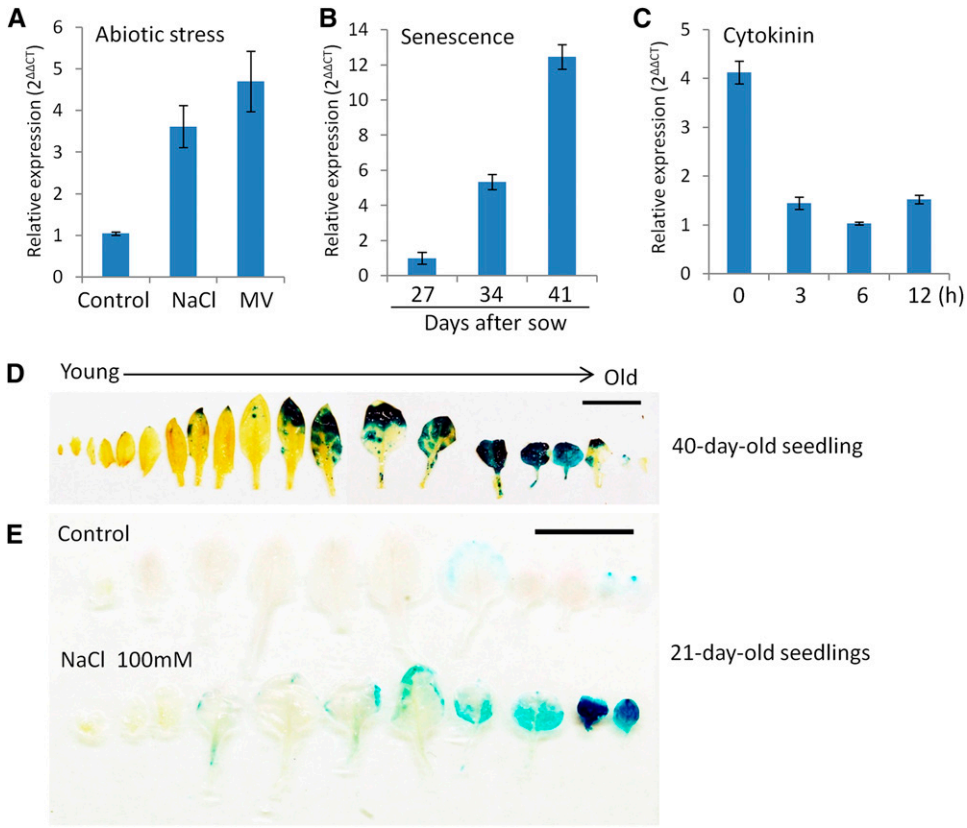

Figure 1. *CV* Expression Is Induced by Senescence and Abiotic Stress.

(A) and **(B)** Quantitative RT-PCR analysis of *CV* gene expression in cassette leaves of the wild type (Col-0) in response to abiotic stress. Ten-day-old seedlings were treated with 100 mM NaCl and 2 μM MV for 2 d **(A)** and during senescence **(B)**.

(C) Quantitative RT-PCR analysis of *CV* gene expression in shoots of 30-d-old Col-0 plants treated with cytokinin (5 μM benzyl adenine) for 0, 3, 6, and 12 h. Error bars in **(A)** to **(C)** show SD ($n = 6$).

(D) and **(E)** GUS staining of cassette leaves from 40-d-old transgenic plants containing ProCV-GUS **(D)** and 16-d-old transgenic plants grown in half-strength Murashige and Skoog (MS) medium without or with 100 mM NaCl for 5 d **(E)**.

and thylakoid membranes appeared swelled and unstacked (Figures 2D and 2E). CCVs were observed attached to the envelope membrane of disassembled chloroplasts (Figure 2E; Supplemental Figure 3A) or protruding from the unstacked thylakoid membranes (Figure 2D). Immunodetection of GFP in cotyledon mesophyll cells of DEX-CV-GFP transgenic plants showed that 87% of the gold particles were localized in chloroplasts and CCVs (Supplemental Figures 3A and 3D). In addition, we analyzed leaf sections from transgenic DEX-CV-HA plants (*DEX-3*) (Supplemental Figure 4) for the double immunolabeling with anti-HA and anti-PsbO1 antibodies. The results showed that the CCVs that are close to, but not associated with, broken chloroplasts also could be labeled by antibodies raised against PsbO1, a subunit of the photosystem II (PSII) complex localized in the thylakoid membrane (Supplemental Figure 4B). Moreover, CCVs also contained Tic20-II, a protein from chloroplast inner envelope membranes (Machettira et al., 2011) (Supplemental Figure 5B). These results suggested that CCVs were generated from chloroplast membranes that were disrupted by CV. These vesicles and disrupted chloroplast structures were not seen in cotyledons from wild-type seedlings (Supplemental Figures 3B and 3C).

CCVs Were Mobilized to the Vacuole through a Pathway Independent of Autophagy and SAVs

The role of autophagy in the mobilization of Rubisco and other stromal proteins to the vacuole is well established (Ohsumi, 2001; Ishida et al., 2008; Bassham, 2009; Wada et al., 2009). During autophagy, cytosolic components and intact or partially broken organelles are engulfed in membrane-bound vesicles called autophagosomes that deliver the vesicle contents to the vacuole for degradation. We transiently expressed the *CV-RFP* fusion in cotyledons from transgenic plants expressing the autophagic marker *GFP-ATG8a* (Thompson et al., 2005). The red fluorescence of CV-RFP did not overlap with the green fluorescence of GFP-ATG8a (Supplemental Figure 6A). Moreover, when CV-GFP was expressed in autophagy-defective *atg5-1*

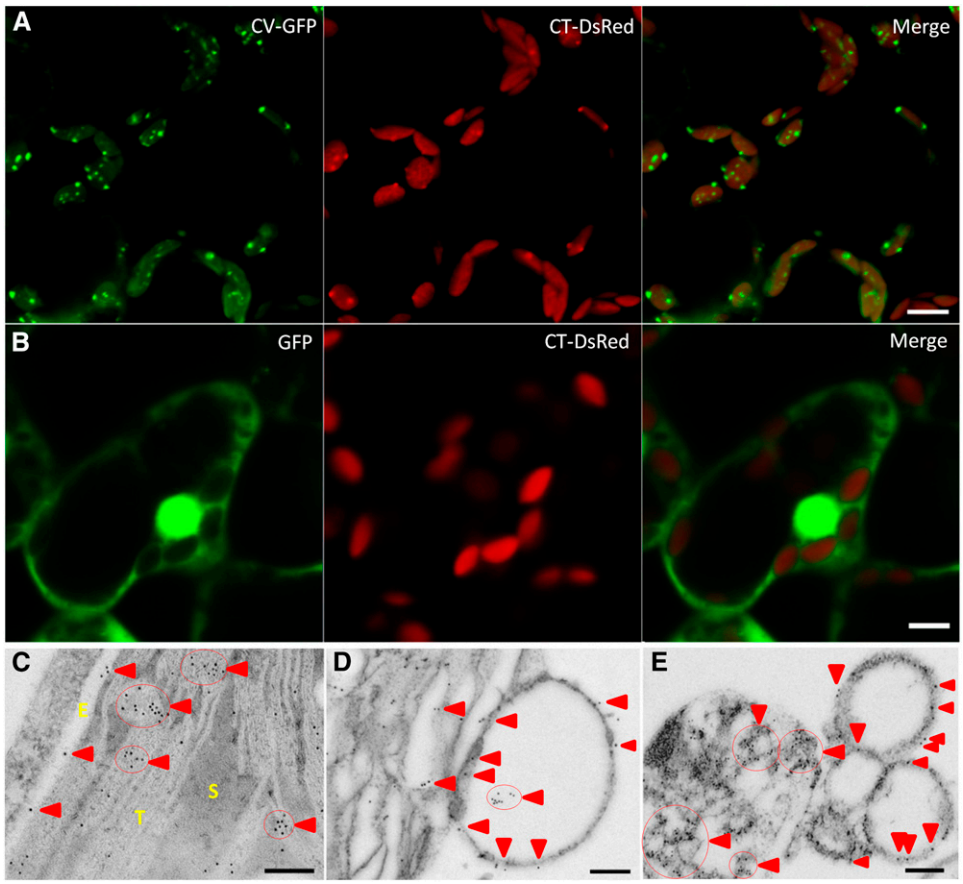

Figure 2. CV-Induced Vesicles Are Released from Chloroplasts.

(A) and **(B)** Transient expression of *CV-GFP* **(A)** and *GFP* **(B)** in cotyledon mesophyll cells from transgenic plants constitutively expressing stroma-targeted DsRed (CT-DsRed). Bars = 10 μm.

(C) to **(E)** Immunodetection of CV-GFP in intact chloroplasts **(C)** and broken chloroplasts (**[D]** and **[E]**) of cotyledon mesophyll cells of DEX-CV-GFP transgenic plants cultured for 24 h in liquid half-strength MS medium containing 10 μM DEX by immunolabeling transmission electron microscopy. Cotyledon sections were immunolabeled with anti-GFP antibodies followed by 10-nm gold-conjugated goat anti-rabbit IgG. E, envelope membrane; S, stroma; T, thylakoid membrane. Red arrowheads indicate the localization of 10-nm gold particles binding to CV-GFP. Red circles indicate the aggregation of CV-GFP. Bars = 200 nm.

mutants (Ishida et al., 2008), CCVs were observed both inside and outside of the chloroplasts (Supplemental Figure 6B), further suggesting that the formation and trafficking of CCVs were independent of autophagy.

During senescence, the formation of small acidic SAVs aids in the degradation of chloroplast proteins. SAVs are formed through a pathway that is independent of autophagy (Otegui et al., 2005; Martínez et al., 2008a; Carrión et al., 2013). To rule out a possible relationship between CCVs and SAVs, we attempted staining cotyledons from plants expressing CV-GFP with LysoTracker Red, a fluorescent dye that stains acidic lytic vesicles including SAVs (Otegui et al., 2005). The lack of CCV staining by LysoTracker Red (Supplemental Figure 7A) indicated that CCV's milieu differed from that of SAVs. In addition, the transient coexpression of *SAG12-RFP* along with *CV-GFP* in cotyledon cells showed that the SAV marker SAG12-RFP did not colocalize with CV-GFP (Supplemental Figure 7B).

A dexamethasone (DEX)-induced promoter was used to express *CV-GFP* (DEX-CV-GFP) in transgenic plants. Stably transformed plants were treated with DEX, and GFP fluorescence was monitored. Six hours after DEX treatment, CV-GFP was seen decorating mesophyll cell chloroplasts and stromules (stroma-filled tubules) (Hanson and Sattarzadeh, 2008, and references therein) extending from the chloroplasts (Figure 3B). Eighteen hours following DEX treatment, the CCVs moved out from the chloroplast along with the stroma-targeted CT-DsRed (Figure 3C). These observations were consistent with the CV transient expression results (Supplemental Figure 1A). Similar results were observed in DEX-induced expression of CV-GFP in true leaf cells (Supplemental Figure 1D) and in cotyledon (Figure 3C) and hypocotyl (Figure 3E) cells; CCVs also could carry CT-DsRed out of chloroplasts and aggregate in cytosols of mesophyll cells of true leaves.

To exclude the possibility that CCVs were produced at the endoplasmic reticulum, DEX-CV-GFP transgenic plants were treated with DEX for 17 h and with concanamycin A, an inhibitor

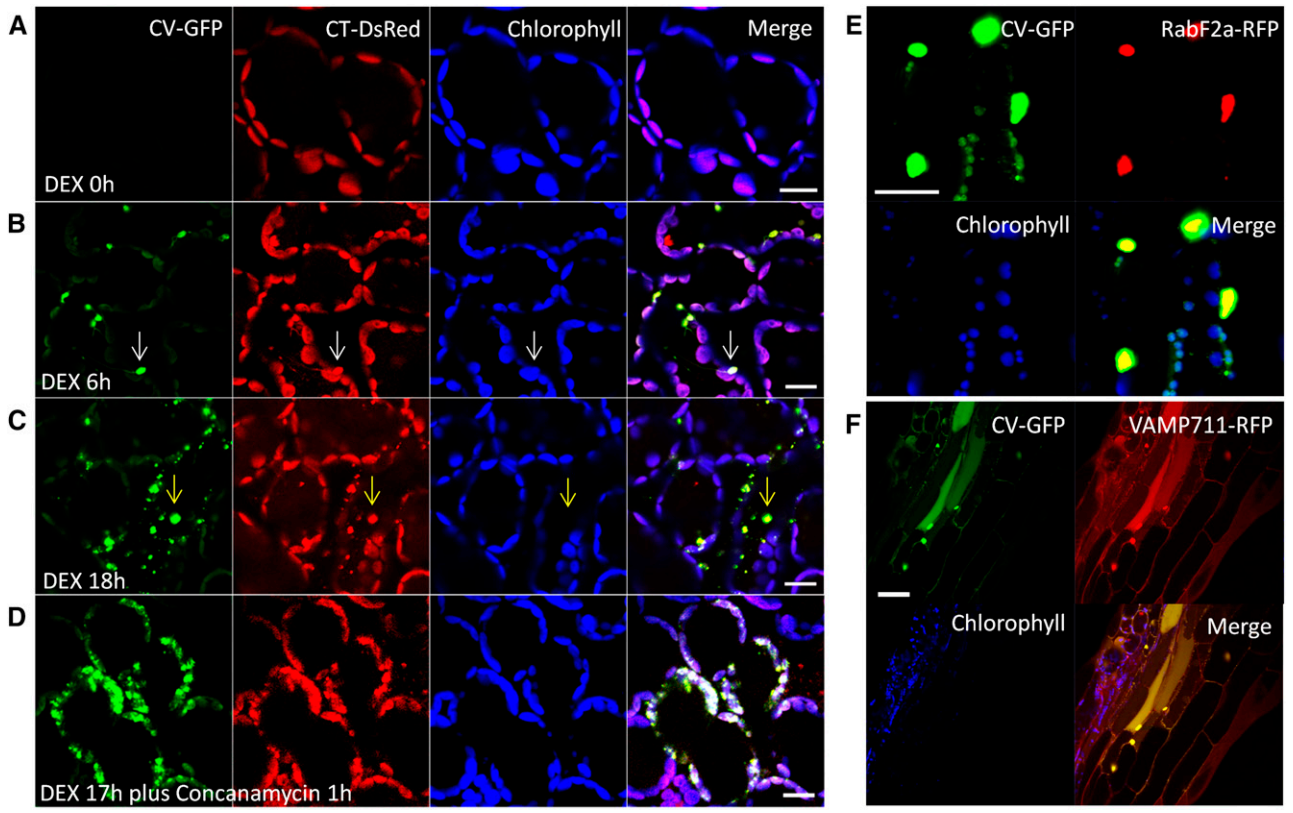

Figure 3. Transport of CV to the Vacuole.

(A) to **(D)** DEX-induced expression in cotyledon mesophyll cells from transgenic DEX-CV-GFP/CT-DsRed plants cultured in liquid half-strength MS medium containing 10 μM DEX for 0 h **(A)**, 6 h **(B)**, 18 h **(C)**, or 17 h plus an additional 1-h treatment with concanamycin **(D)**. White arrows in **(B)** represent the stromule extending from a chloroplast labeled by CV-GFP. Yellow arrows in **(C)** indicate the CCV released from chloroplasts. Bars = 10 μm.

(E) and **(F)** Transient expression of CV-GFP in hypocotyl cells of transgenic plants constitutively expressing the prevacuolar compartment RabF2a-RFP **(E)** and a tonoplast R-SNARE, VAMP711-RFP **(F)**. Bars = 20 μm.

of intracellular vesicle trafficking (Dettmer et al., 2006), for an additional 1 h. The CCVs appeared to adhere to the chloroplasts after treatment (Figure 3D), suggesting that concanamycin A treatment inhibited the release of CCVs from chloroplasts.

To assess whether CCVs were eventually transported to the vacuole, the *CV-GFP* was transiently expressed in stable reporter lines containing *Rab2a-RFP*, a prevacuolar compartment rab5 GTPase Rha1 (Foresti et al., 2010), and *VAMP711-RFP*, a tonoplast R-SNARE (Uemura et al., 2004). Localization results showed that CV-GFP overlapped with RabF2a-RFP and VAMP711-RFP in hypocotyls cells (Figures 3E and 3F) 3 d after transient expression, supporting the mobilization of CCVs to the central vacuole.

CV Overexpression Led to Chloroplast Degradation

Attempts to overexpress CV under the control of the CaMV35S constitutive promoter were not successful, suggesting that the high CV expression was lethal. Alternatively, we used a chemically inducible expression system to drive the expression of *CV-HA*. Phenotypic analysis of three independent stable lines, *DEX-1*, *DEX-2*, and *DEX-3* (Figure 4A), showed that DEX-induced CV expression resulted in leaf chlorosis and overall growth retardation (Figure 4B). Following DEX treatment, leaf chlorophyll content decreased as compared with untreated transgenic and wild-type plants (Figure 4C). Immunoblot analyses in DEX-treated plants revealed degradation of the photosystem I (PSI) complex subunit PsaB, PSII subunits (11 and D1), and stromal protein glutamine synthase 2 (GS2). The levels of cytosolic sucrose phosphate synthase (SPS) remained unchanged upon DEX treatment (Figure 4D), whereas the abundance of cytosolic glutamine synthase 1 (GS1) increased, consistent with a previous study showing the upregulation of GS1 expression during senescence (Bernhard and Matile, 1994). Oxidative stress, induced by the exposure of the plants to 0.3 μM MV, enhanced stress-induced chloroplast degradation in transgenic plants expressing *CV* (Figures 4B and 4C). Overexpression of *CV-GFP* also induced the accelerated senescence phenotype in the presence of 50 mM NaCl (Supplemental Figure 8). These results indicated that the overexpression of CV lead to premature senescence and chloroplast degradation.

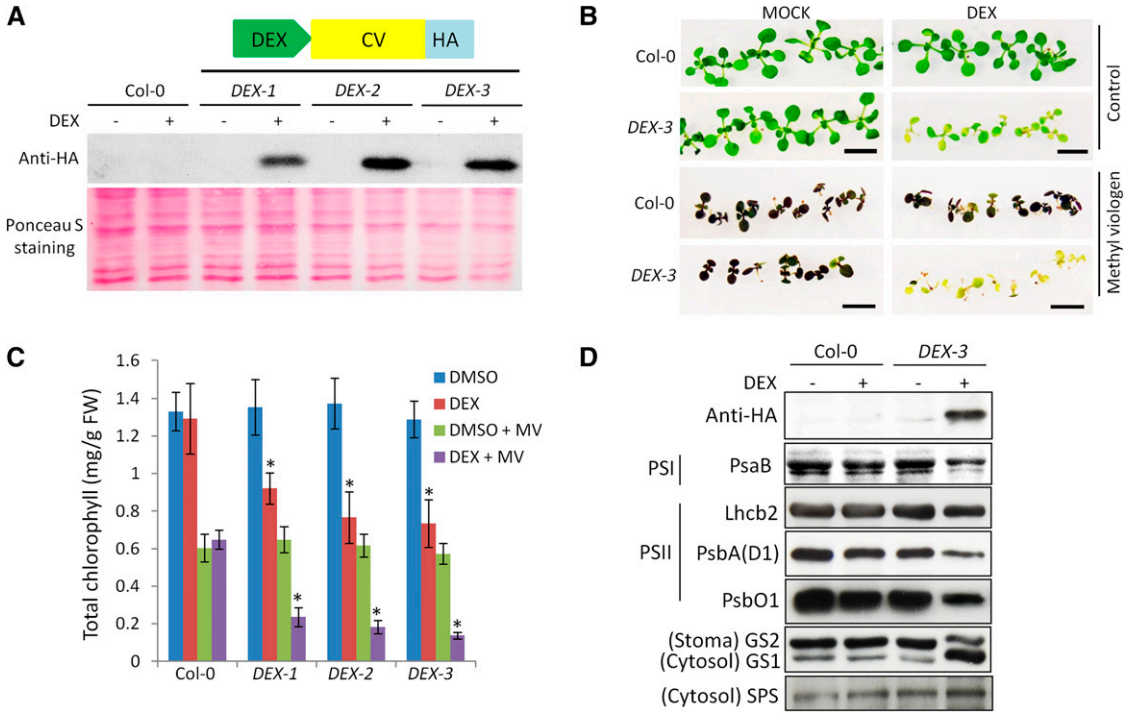

Figure 4. Overexpression of *CV* Resulted in Chloroplast Degradation.

(A) Immunoblot analysis of DEX-induced expression of CV-HA. Analyses used an anti-HA antibody in the wild type (Col-0) and three independent transgenic lines of DEX-CV-HA (*DEX-1*, *DEX-2*, and *DEX-3*). Ponceau S staining indicates the equal loading of total protein extractions for immunoblot analysis.

(B) and **(C)** Morphology **(B)** and total chlorophyll contents **(C)** of wild-type Col-0 and transgenic plants (*DEX-1*, *DEX-2*, and *DEX-3*) after combined treatments of DEX and MV. Four-day-old seedlings were transferred to half-strength MS medium in the absence or presence of DEX or MV or a combination of both and cultured for 1 week. All the leaves and cotyledons of plants were used for chlorophyll measurement. Mean ± SD values were obtained from three independent experiments. Asterisks indicate significant differences at $P < 0.001$ from Col-0 for each treatment. FW, fresh weight. Bars = 1 cm.

(D) Immunoblot analysis of CV-HA, chloroplast proteins, and cytosol proteins in Col-0 and DEX-3 plants with or without DEX treatment. Chloroplast proteins include PSI subunit PsaB, PSII subunits Lhcb2, PsbA (D1), and PsbO1, and stromal protein GS2. Cytosol proteins are GS1 and SPS.

CV Silencing Caused Delayed Chloroplast Degradation

An artificial microRNA targeting *CV* (*amiR-CV*) was designed using WMD3 (http://wmd3.weigelworld.org/cgi-bin/webapp.cgi) (Schwab et al., 2006), and its expression was driven by the *CaMV35S* promoter. Three independent transgenic lines (*amiR-CV1-3*) were selected, and *CV* silencing was examined by quantitative RT-PCR (Figure 5A). CV-silenced plants had no apparent developmental defects, and their natural senescence was also indistinguishable from that of wild-type plants (Supplemental Figure 9A). However, when 20-d-old seedlings of wild-type and *amiR-CV* plants were treated with increasing NaCl concentrations (Figure 5C), the wild-type plants displayed severe leaf senescence symptoms, while the *amiR-CV* plants remained green (Figure 5B). Chlorophyll content decreased in wild-type cassette leaves during the treatment, whereas salt stress-induced leaf senescence was delayed in CV-silenced plants (Figure 5C). The degradation of PSI subunits (PsaB), PSII subunits (D1, PsbO1, and Lhcb2), and stroma protein GS2 were evident in wild-type plants after 10 d of salt treatment (Figure 5D). In *amiR-CV* plants, the abundance of the above-mentioned chloroplast proteins decreased only slightly after 16 d of salt treatments (Figure 5D). These results demonstrated that silencing *CV* inhibited the salt stress-induced degradation of chloroplast proteins. In addition, the chloroplast degradation caused by MV-induced oxidative stress (Supplemental Figures 9B and 9C) was also delayed in *amiR-CV* lines. Moreover, their survival rates increased significantly after a 14-d drought treatment (Supplemental Figure 10). These results indicated that silencing *CV* increased chloroplast stability and prevented abiotic stress-induced senescence.

The C-Terminal Domain of CV Is Important for Chloroplast Destabilization and the Formation of CCVs

A search for sequences similar to *CV* in the public genome databases showed the presence of *CV* homologs in all plant species sequenced so far (Supplemental Figure 2). These genes encode a unique highly conserved domain at the C terminus of the respective proteins (Figure 6A; Supplemental Figure 2).

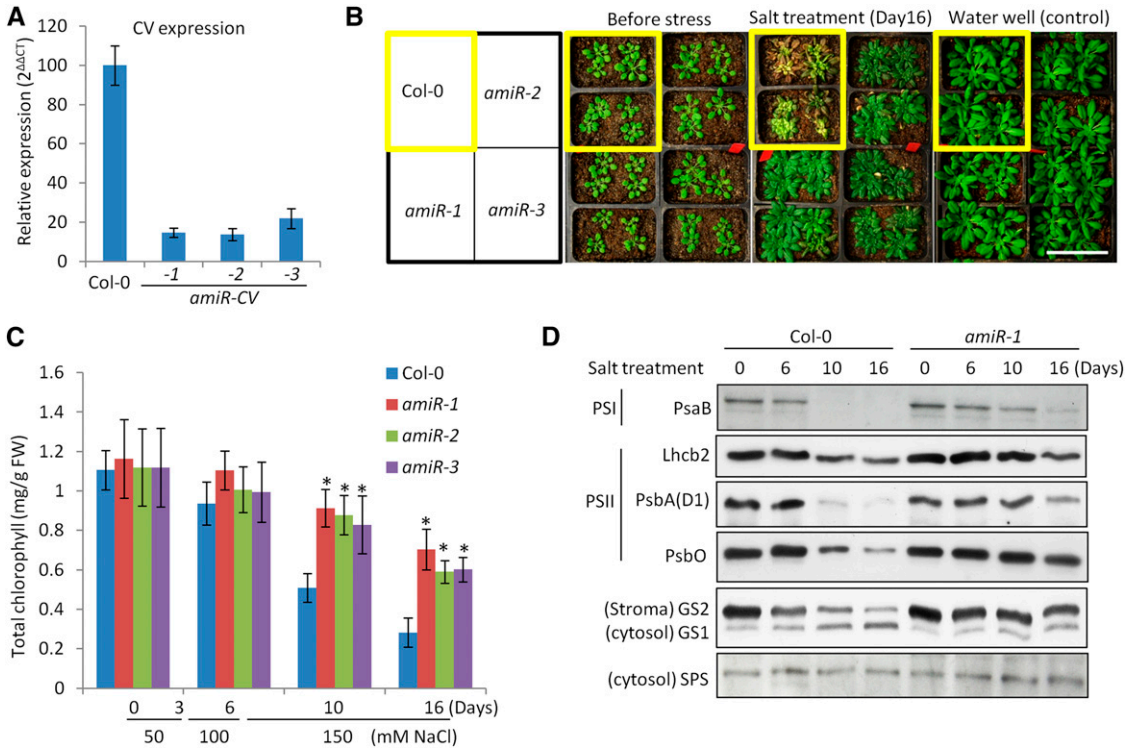

Figure 5. Artificial MicroRNA Silencing of *CV* Delayed Salt Stress-Induced Chloroplast Degradation.

(A) Quantitative RT-PCR analysis of CV expression in all leaves from 30-d-old plants of Col-0 and three independent artificial microRNA-silenced lines of CV (*amiR-1*, *amiR-2*, and *amiR-3*).

(B) and **(C)** Morphology **(B)** and leaf chlorophyll content **(C)** of Col-0 and three independent CV-silenced lines (*amiR-1*, *amiR-2*, and *amiR-3*) during salt stress treatment (50 mM NaCl for 3 d, 100 mM NaCl for 3 d, and 150 mM NaCl for 10 d). Chlorophyll was extracted from leaf tissues. Mean ± SD values were obtained from three independent experiments. Asterisks indicate significant differences at $P < 0.001$ from Col-0 for each treatment. FW, fresh weight.

(D) Immunoblot analysis of chloroplast proteins and cytosolic proteins in leaves from Col-0 and *amiR-1* plants during salt stress treatment as described in **(C)**. Chloroplast proteins include PSI subunit PsaB, PSII subunits Lhcb2, PsbA (D1), and PsbO1, and stromal protein GS2. Cytosol proteins are GS1 and SPS.

Without the conserved C-terminal domain, CVΔC-GFP was still localized at the chloroplasts but barely produced vesicles, as indicated in the bottom row of Figure 6B. Moreover, the DEX-induced expression of *CVΔC-GFP* produced some leaf senescence (Figure 6C) and partial chloroplast degradation (Figure 6D). Nonetheless, the destabilizing functions of CVΔC-GFP were substantially impaired as compared with the plants expressing the full-length CV-GFP (Figures 6C and 6D), indicating a key role of the conserved C-terminal domain of CV in chloroplast destabilization and the formation of CCVs.

CV Interacts with PSII Subunit PsbO in Vivo

To elucidate the mechanism(s) by which CV disrupts chloroplasts, we identified potential CV-interacting proteins using coimmunoprecipitation (co-IP) and subsequent identification of interactors by liquid chromatography-tandem mass spectrometry (LC-MS/MS) (Smaczniak et al., 2012). Antibodies raised against HA were conjugated to magnetic beads, and these beads were used to immunoprecipitate CV-HA and its interacting proteins from total protein extracts obtained from DEX-treated transgenic plants expressing *DEX-CV-HA* (*DEX-3* line). Protein extracts from wild-type Columbia-0 (Col-0) plants were used as a control to detect proteins that bind nonspecifically to the anti-HA beads. Most of the immunoprecipitated proteins were chloroplast proteins, including PSII complex subunits, NAD(P)H dehydrogenase subunits, thylakoid membrane-bound proteases, and a few stromal proteins (Supplemental Table 1). The similarity between the peptide abundances of PSII subunits 1, PsbO2, and the bait protein CV (Supplemental Table 1) and their localization and functions indicates an interaction between CV and PsbO proteins. In order to confirm this interaction, we used bimolecular fluorescence complementation (BiFC). The transient expression of both fusion genes *CV-SCFP^C* and *PsbO1-Venus^N* in cotyledons of wild-type seedlings resulted in BiFC fluorescence that was seen not only in the chloroplasts but also in the CCVs (Figure 7A). By contrast, the coexpression of *CV-SCFP^C* and *SGR1-Venus^N* failed to produce green fluorescence signals in three independent tests (Figure 7C). These results indicated a direct interaction between CV and PsbO1 in vivo. Interestingly, coexpression of the N-terminal fusion *SCFP^C-PsbO1* and *Venus^N-CV* also induced

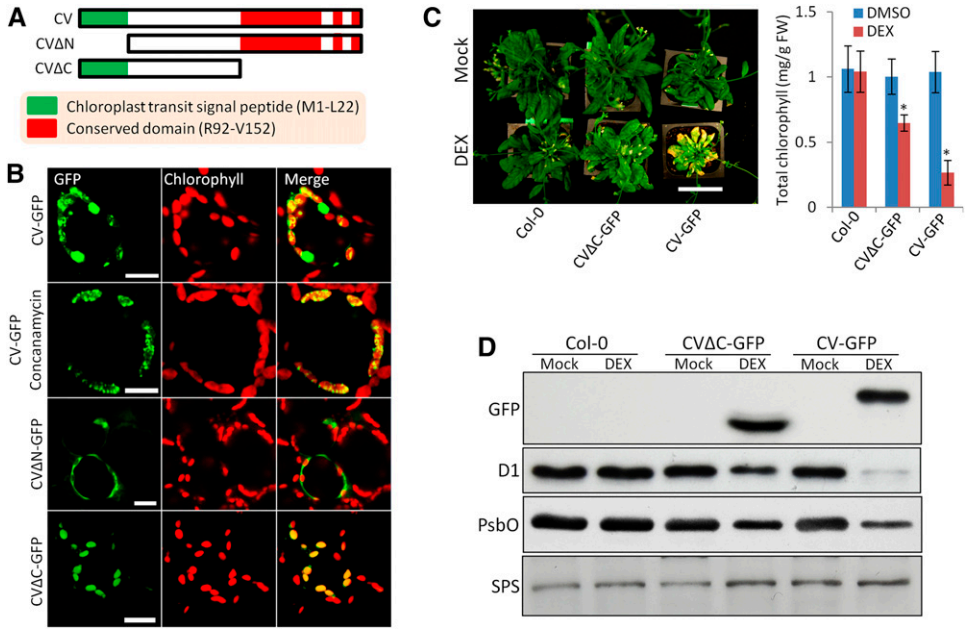

Figure 6. The C-Terminal Conserved Domain of CV Is Necessary for Chloroplast Destabilization.

(A) Schematic diagram showing the putative functional domains of CV. The green boxes represent the chloroplast transit signal peptide, and the red boxes represent the C-terminal conserved domain. CVΔN has a deletion of the N-terminal chloroplast transit signal peptide. CVΔC has a deletion of the C-terminal conserved domain.

(B) Transient expression of constructs *CV-GFP*, *CVΔN-GFP*, and *CVΔC-GFP* in cotyledon mesophyll cells of wild-type plants. The cotyledon expressing *CV-GFP* was cultured in liquid half-strength MS medium containing concanamycin for 1 h. Bars = 10 μm.

(C) Morphology and leaf chlorophyll content of 45-d-old plants of wild-type Col-0, transgenic DEX-CVΔC-GFP, and DEX-CV-GFP after watering with 10 μM DEX or DMSO (Mock) for 3 weeks. Chlorophyll was extracted from leaf tissues. Mean ± SD values were obtained from three independent experiments. Asterisks indicate significant differences from mock treatment at $P < 0.001$. FW, fresh weight.

(D) Immunoblot analysis of GFP, chloroplast proteins D1 and PsbO, and cytosolic protein SPS in leaves from 45-d-old plants of wild-type Col-0, transgenic DEX-CVΔC-GFP, and DEX-CV-GFP plants following chemical treatments as described in **(C)**.

fluorescence, but it was not associated with chloroplasts (Figure 7D). This suggests that the N-terminal fusion did not affect the interaction between CV and PsbO1 but misdirected proteins to locations (perhaps cytosol) other than the chloroplast because of the disruption of the N-terminal chloroplast transit signal peptide of CV and PsbO1.

We also constructed another mutation, CVΔC, by deleting the conserved C-terminal domain of CV. No fluorescence was detected between *CVΔC-SCFP^C* and *PsbO1-Venus^N* (Figure 7B). These results indicated that the conserved C-terminal domain was required for the interaction between CV and PsbO1.

This was further confirmed by the co-IP results showing that full-length CV, but not CVΔC, was immunoprecipitated by an anti-PsbO1 antibody (Figure 7E). In addition, we transiently coexpressed *CV-YFP* together with *PsbO1-CFP* in wild-type seedlings. In cells without CV-YFP, PsbO1-CFP was distributed uniformly in chloroplasts (Figure 7F). However, *CV-YFP* expression altered the localization of PsbO1 and caused the concentration of PsbO1-CFP in the CCVs (Figure 7G). Collectively, these findings suggested that CV could disrupt the localization of PsbO1 in chloroplasts, possibly through direct protein-protein interaction.

In addition to the stroma-targeted DsRed and PSII subunit PsbO1, we also observed two more thylakoid proteins decorated with CCVs. The gene encoding the thylakoid lumen protein AtCYP20-2, an immunophilin associated with the PSI/NDH supercomplex (Sirpiö et al., 2009), was cloned and fused with *CFP*. *CYP20-CFP* was coexpressed transiently with *CV-GFP* in cotyledons, and confocal microscopy observations clearly showed their colocalization (Supplemental Figure 11A). Also, the gene encoding the thylakoid membrane-bound FtsH protease was fused to *CFP*, and the *AtFtsH1-CFP* was coexpressed with *CV-GFP*. Our results showed that AtFtsH1-CFP and CV-GFP were both present in chloroplast and in CCVs released from the chloroplast (Supplemental Figure 11B). However, the plastoglobule marker protein plastoglobulin 34, PGL34-YFP (Vidi et al., 2007), did not overlap with CV-RFP (Supplemental Figure 11C), suggesting that plastoglobule turnover was independent of the CV-induced degradation pathway.

DISCUSSION

CV Regulates Stress-Induced Chloroplast Degradation through a Pathway Independent of Autophagy and SAVs

Plants use different strategies to cope with environmental stress. The escape strategy involves the rapid degradation of

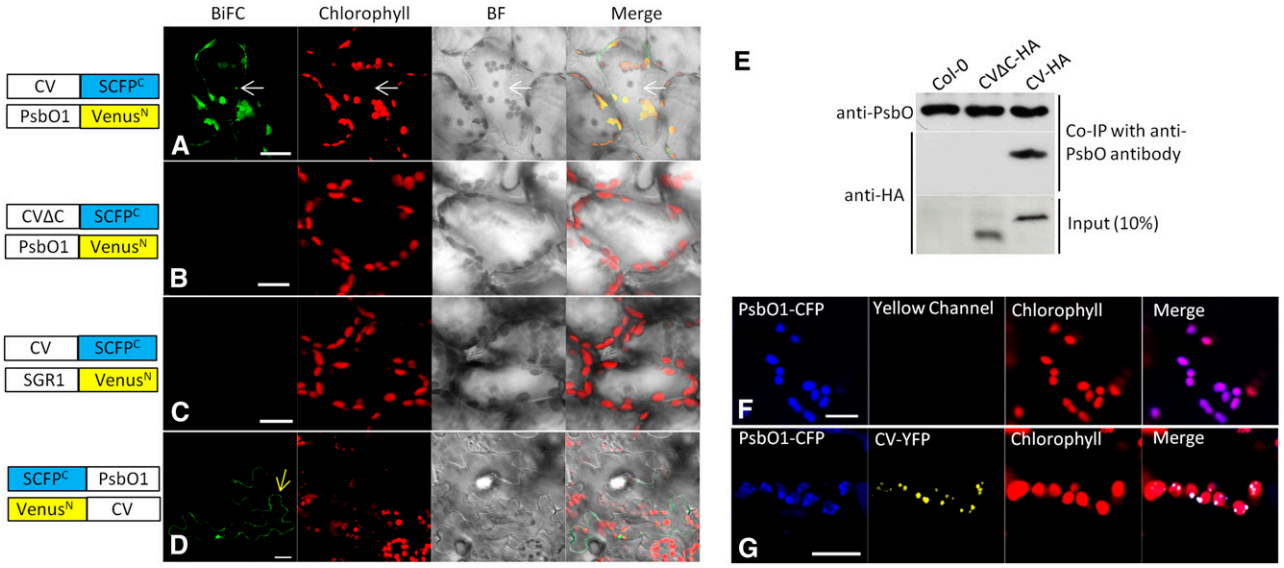

Figure 7. CV Interacts with the PSII Subunit PsbO1 in Vivo.

(A) to **(D)** BiFC analysis of in vivo interactions: CV-SCFP^C and PsbO1-Venus^N **(A)**, CVΔC-SCFP^C and PsbO1-Venus^N **(B)**, CV-SCFP^C and SGR1-Venus^N **(C)**, and SCFP^C-PsbO1 and Venus^N-CV **(D)**. White arrows indicate the vesicle outside the chloroplast. BiFC, green fluorescence from interacting SCFP^C and Venus^N; Chlorophyll, autofluorescence of chlorophyll. Bars = 20 μm.

(E) Co-IP of PsbO with HA-tagged CV and CVΔC. Crude lysates (Input) from wild-type Col-0 without or with transient expression of CV-HA and CVΔC were immunoprecipitated with an anti-PsbO antibody. Co-IP samples were detected by immunoblotting with an anti-PsbO or anti-HA antibody, respectively.

(F) and **(G)** Confocal microscopy observations of cotyledon mesophyll cells from transiently expressing PsbO1-CFP **(F)** and coexpressing PsbO1-CFP and CV-YFP **(G)**. Bars = 10 μm.

source tissues and the accelerated development of sinks, contributing to a more rapid production of seeds for the next generation (Levitt, 1972). Chloroplasts contain large amounts of proteins, and the rapid and massive chloroplast degradation during stress is a key process that provides nutrients for relocation to developing organs (Makino and Osmond, 1991). In this study, we identified *CV*, which encodes a protein that mediates the turnover of chloroplast proteins. Our results showed not only that silencing of *CV* delayed the stress-induced chloroplast degradation and leaf senescence but also that *CV* overexpression caused chloroplast degradation and premature leaf senescence (Figures 4B and 5B; Supplemental Figures 8A and 9B).

Previous studies revealed two extraplastidic proteolytic processes, autophagy (Ishida et al., 2008; Wada et al., 2009) and SAVs (Otegui et al., 2005; Martínez et al., 2008a; Carrión et al., 2013), that are involved in the degradation of chloroplasts. However, little is known about the factors regulating intraplastidic chloroplast degradation. Our results revealed a proteolytic pathway that is independent of autophagy and SAVs and is mediated by the formation of CCVs. We present a model (Supplemental Figure 12) showing how *CV* expression can be elicited by tissue senescence or stress-induced senescence (Figures 1A and 1B). After targeting to the chloroplast, CV induces the formation of vesicles in chloroplasts (CCVs) (Figure 2A) through a mechanism that is as yet unclear. The CCVs are eventually released from the chloroplast (Supplemental Figure 1C) to the cytosol, carrying away some cargo proteins from the chloroplast (Figure 3C). In addition to stromal protein, CCVs were shown to contain the thylakoid membrane protein FtsH1 (Supplemental Figure 11B), the lumenal proteins PsbO1 (Figure 7G) and AtCYP20-2 (Supplemental Figure 11A), and the inner envelope membrane protein Tic20-II (Supplemental Figure 5B).

Based on the immunolabeling results, CV proteins are primarily associated with thylakoid membranes and envelope membranes prior to the formation of CCVs (Figure 2G), likely via its putative transmembrane domain (Supplemental Figure 2). Confocal microscopy observations also demonstrated the colocalization of CV and the inner envelope membrane protein Tic20-II (Supplemental Figure 5B). Although the exact mechanism of vesicle formation remains elusive, these results, together with our observations showing that the CV-induced vesicle formation was coupled with the unstacking and swelling of the thylakoid membranes and the disassembling of the chloroplast structure (Figures 2D and 2E), support the notion that the CCVs form directly from the chloroplast membranes that are disrupted by CV (Figure 2D; Supplemental Figure 4B).

Autophagy induces the formation of RCBs by engulfing the stromules protruding from chloroplasts, and the chloroplast functions are still maintained (Ishida et al., 2008). As compared with autophagy-dependent degradation, CV-mediated degradation appears to be more destructive. CV-mediated chloroplast damage leads to leaf senescence, as observed during DEX-induced *CV* overexpression (Figure 4). Interestingly, silencing *CV*

did not delay natural leaf senescence. A possible explanation of this phenomenon is that other pathways, such as autophagy (Ishida et al., 2008; Wada et al., 2009), SAVs (Otegui et al., 2005; Martínez et al., 2008a; Carrión et al., 2013), and SGR-mediated chlorophyll degradation (Park et al., 2007; Ren et al., 2007; Hörtensteiner, 2009; Sakuraba et al., 2012), are enhanced in *CV*-silenced plants for destabilizing chloroplasts and accelerating senescence. The possible interactions between the processes of autophagy, SAVs, and CV-dependent degradation are unknown and require further investigation.

CV Mediates Chloroplast Destabilization and Vesiculation

Co-IP and subsequent analysis by LC-MS/MS revealed several proteins that potentially interact with CV (Supplemental Table 1). We confirmed that CV interacts with the PSII subunit PsbO1 in vivo by BiFC assays (Figure 7). Another PsbO gene product, PsbO2, which shares 91% similarity with PsbO1 in amino acid sequence, was also immunoprecipitated by CV (Supplemental Table 1), suggesting the CV-PsbO2 interaction.

In addition to its role in stabilizing manganese, PsbO is thought to play a chaperone-like role in PSII assembly (Yamamoto, 2001; Yamamoto et al., 2008). Although the functions of PsbO1 and PsbO2 are not completely redundant (Lundin et al., 2007), RNA interference silencing of both genes (Yi et al., 2005) leads to decreased stability of PSII and the loss of some photosynthetic proteins, including CP47, CP43, D1, and the PSI core protein PsaB. By contrast, LHCII was stable in PsbO RNA interference lines (Yi et al., 2005). In CV-overexpressing lines, D1 and PsaB were degraded, but the stability of Lhcb2 was less affected as compared with other PSII proteins (Figure 4D). Furthermore, CP43 and D1 were also immunoprecipitated by CV (Supplemental Table 1).

Altogether, these results strongly suggested the functional interaction between CV and PsbO. CV targeted PsbO directly and might alter the structure of the PSII complex, removing PsbO (Figure 7G), affecting PSII stability, and making core proteins (such as D1) more susceptible to thylakoid proteases. The proteases Deg (Kapri-Pardes et al., 2007) and FstH (Lindahl et al., 2000; Zaltsman et al., 2005; Shen et al., 2007; Adam et al., 2011) have been identified to be responsible for the turnover of D1. Interestingly, both DegP1 and FstH1 appeared to interact with CV (Supplemental Table 1), and FstH1-CFP colocalized with CV-GFP in vivo (Supplemental Figure 11B). Taken together, these results suggest a mechanism by which CV might facilitate the approach of proteases to D1 protein after removing PsbO. CV-dependent removal of PsbO promotes PSII turnover and destabilizes chloroplasts.

In addition, previous in vitro studies revealed that the aggregation of D1 and other subunits, including CP43, occurred in the absence of PsbO (Henmi et al., 2003; Yamamoto et al., 2008). Thus, CV-induced elimination of PsbO could cause the aggregation of D1 with other PSII core proteins, and this aggregation could be a signal for vesicle formation. Supporting this notion, it has been shown recently that the overexpression of *Triple Gene Block3* (*TGB3*) of *Alternanthera mosaic virus* in *Nicotiana benthamiana* caused chloroplast vesiculation and veinal necrosis by interacting with the host PsbO (Jang et al., 2013). CV interacts with PsbO1 via a C-terminal domain that is highly conserved in the plant kingdom (Supplemental Figure 2). The conserved domain appeared to be important for vesicle formation and chloroplast degradation (Figure 6). However, deletion of this conserved domain did not completely eliminate chloroplast function (Figure 6). Several chloroplast proteins, in addition to PsbO, were also immunoprecipitated by CV, suggesting that PsbO1 may not be the only protein targeted by CV during the process of chloroplast degradation.

Stress Tolerance Is Increased by Stabilization of the Chloroplasts

Abiotic stress limits plant growth and productivity by disrupting photosynthesis and inducing senescence. Emerging evidence suggests that chloroplast stability plays a significant role in the tolerance of plants to abiotic stress. Senescence and stress-induced synthesis of cytokinin synthesis delay the degradation of photosynthetic complexes in transgenic plants expressing P_{SARK}-*IPT*, which displayed enhanced drought tolerance (Rivero et al., 2010). In addition, a wheat (*Triticum aestivum*) stay-green mutant (*tasg1*) displays delayed chlorophyll turnover and improved tolerance to drought because of the enhanced stability of thylakoid membranes (Tian et al., 2013). The stable chloroplasts also could contribute to maintain photorespiration, which has been shown to increase tolerance to abiotic stress by protecting the photosynthetic apparatus from oxidative damage and optimizing photosynthesis (Rivero et al., 2009; Voss et al., 2013). Here, we showed that silencing of *CV* increased chloroplast stability and prevented premature senescence under salt, oxidative, and drought stress (Figure 5; Supplemental Figures 9B and 10). Our results indicate that CV may act as a scaffold targeting PSII proteins directly. Thus, silencing *CV* may protect PSII functions, increasing plant tolerance to abiotic stress. Moreover, CV-silenced plants displayed increased GS2 stability (Figure 5D). GS2 is a major enzyme for nitrogen assimilation, and *GS2* overexpression leads to increased salt stress tolerance in rice (Hoshida et al., 2000).

In conclusion, our results provide evidence supporting a pathway for the degradation of thylakoid and stromal proteins that is independent of autophagy (Ishida et al., 2008) and SAVs (Otegui et al., 2005; Martínez et al., 2008a; Carrión et al., 2013). Whereas autophagy is responsible for general cellular degradation, CV appears to be unique and specific for chloroplast degradation. From a biotechnological perspective, silencing of CV offers a suitable strategy for the generation of transgenic crops with increased tolerance to abiotic stress.

METHODS

Plant Materials and Growth Conditions

Arabidopsis thaliana (Col-0) plants were grown in a growth chamber at 23° C under 100 μmol m^{-2} s^{-1} light in a 16-h-light/8-h-dark regime. MS/2 medium (0.5% sucrose, pH 5.7) was used for plate-grown plants. Transgenic *Arabidopsis* plants expressing stroma-targeted DsRed (CT-DsRed) were generated as described previously (Ishida et al., 2008). The generation of transgenic plant GFP-ATG8a (Thompson et al., 2005), the autophagy-defective mutant *atg5-1* (Ishida et al., 2008), the vacuole

marker line VAMP711-RFP (Uemura et al., 2004), and the plastoglobule marker line PGL34-YFP (Vidi et al., 2007) was performed as described previously.

All the constructs in this study were generated using the Gateway system (Invitrogen). The cDNA of AtCV (At2G25625) was amplified from mature leaf cDNA of Col-0. The 3′ terminus of the *AtCV* gene was fused with *GFP* by fusion PCR, and a linker (GGAAGGAA) was introduced between *AtCV* and *GFP*. The single *AtCV* gene and the fusion fragment (*CV-linker-GFP*) were both cloned into *pDONR207* by BP reaction. *pDONR207-CV* was recombined via LR reaction into the following destination vectors: pEarley-Gate 101 (Earley et al., 2006) for YFP fusion (*CV-YFP*), pB7RWG2 (https://gateway.psb.ugent.be/search) for RFP fusion (*CV-RFP*), and a chemical-inducible system, *pBAV154* (Vinatzer et al., 2006), for stable transformation (*DEX-CV-HA*). The *pDONR207-AtCV-linker-GFP* was recombined into pEarley-Gate 100 for transient expression (*CV-GFP*) and into *pBAV154* for chemically-induced stable transformation (*DEX-AtCV-GFP*). An artificial microRNA (TTACACGTAATGAACTTCCAG) targeting AtCV (*amiR-CV*) was designed with WMD3 (http://wmd3.weigelworld.org/cgi-bin/webapp.cgi) and cloned (Schwab et al., 2006) into pEarley-Gate 100 for stable transformation. Using the same strategy, the genes of *AtPsbO1* (At5G66570), *AtCYP20-2* (At5G13120), and *FtsH1* (At1G50250) were fused with CFP first and then recombined into pEarley-Gate 100 to obtain constructs *PsbO1-CFP*, *CYP20-2-CFP*, and *FtsH1-CFP*, respectively. Deletion mutagenesis to remove either the chloroplast transit signal peptide (M1-L22) or the C-terminal conserved domain (R92-V152) was performed by PCR, and the mutated fragments were fused with *GFP* and recombined into pEarley-Gate 100 to generate constructs *CVΔN-GFP* and *CVΔC-GFP*, respectively. Transient expression was performed in cotyledons of Col-0 young seedlings as described previously (Marion et al., 2008). Stable transformation was performed according to the floral dipping method (Clough and Bent, 1998). A list of primers is included in Supplemental Table 2.

RNA Extraction and Quantitative RT-PCR

To assess senescence-induced CV expression, total RNA was extracted from cassette leaf 7 of Col-0 plants growing in soil under 16 h of light and 8 h of dark. For testing abiotic stress-induced CV expression, total RNA was extracted from all the leaves of 10-d-old seedlings growing without (control) or with 100 mM NaCl or 2 μM MV for 2 d. For assessing artificial microRNA silencing of CV, cassette leaf 7 from 30-d-old plants of Col-0 and *amiR-CV* lines was used for total RNA extraction. Total RNA was extracted by using the RNeasy Mini Kit (Qiagen) with three biological replicates. First-strand cDNA was synthesized from 1 μg of total RNA with the QuantiTech reverse transcription kit (Qiagen). Quantitative PCR was performed on the StepOnePlus (Applied Biosystems) using SYBR Green (Bio-Rad). The $2^{-\Delta\Delta CT}$ method (Livak and Schmittgen, 2001) was used to normalize and determine the mRNA level relative to an internal reference gene, TIP41-like family protein. All the primers are included in Supplemental Table 2.

Fluorescence and Confocal Microscopy

Fluorescence microscopy was performed using an inverted Zeiss LSM 710 confocal laser scanning microscope (Carl Zeiss) equipped with a 40× water-immersion objective. The excitation wavelength/emission were as follows for GFP (488 nm/500 to 530 nm), CFP (440 nm/460 to 490 nm), YFP (514 nm/525 to 552 nm), DsRed (543 nm/575 to 625 nm), LysoTracker Red (561 nm/570 to 600 nm), RFP (561 nm/600 to 660 nm), and chlorophyll (633 nm/650 to 720 nm). To avoid overlap between the fluorescence channels, sequential scanning was used when necessary. Images were processed by ImageJ (http://rsbweb.nih.gov/ij/) and assembled by Photoshop software (Adobe).

Immunolabeling Transmission Electron Microscopy

Ten-day-old seedlings of *DEX-CV-GFP* transgenic plants and Col-0 were cultured in liquid MS/2 medium containing 10 μM DEX for 20 h. The cotyledons were observed by confocal microscopy, and the tissues with high expression of CV-GFP were fixed in paraformaldehyde (2%) and glutaraldehyde (2.5%) as described previously (Shipman and Inoue, 2009). Immunolabeling was performed on ultrathin sections on formvar-coated grids using an anti-GFP antibody (Novus Biologicals) and a goat anti-rabbit secondary antibody conjugated with 10-nm gold particles (British BioCell International). All the grids were stained with uranyl acetate and lead citrate before being observed on a Phillips CM120 Biotwin. Images were taken with a Gatan MegaScan digital camera (model 794/20). For the double immunolabeling experiments, leaf sections from the transgenic line DEX-CV-HA (*DEX-3*) were immunoblotted with anti-HA antibody (from mouse) and anti-PsbO antibody (from rabbit), then treated subsequently with 5-nm gold-conjugated goat anti-mouse IgG and 20-nm gold-conjugated goat anti-rabbit IgG for 1 h. The grids were stained with uranyl acetate and lead citrate for observation.

Immunoblot Analyses

Plant leaf tissues were weighed, frozen in liquid N_2, and ground in three volumes of 2× Laemmli sample buffer. Total proteins were separated by SDS-PAGE, transferred to a polyvinylidene difluoride membrane (Bio-Rad), and probed as described previously (Wang et al., 2011). Monoclonal antibodies raised against the HA tag were purchased from Covance (MMS-101P). Antibodies raised against PsbO (AS05092), SPS (AS03035A), PsaB (AS06166A), PsbA/D1 (AS01016), GS1/GS2 or GLN1/GLN2 (AS08295), and Lhcb2 (AS01003) were obtained from Agrisera. Horseradish peroxidase-conjugated secondary antibodies were purchased from Santa Cruz Biotechnology.

Immunoprecipitation and LC-MS/MS

Four-day-old seedlings of Col-0 and transgenic *DEX-CV-HA-3* plants (*DEX-3*) were cultured in MS/2 medium containing 10 μM DEX for 4 d and then kept in the dark for an additional 2 d. The shoots of plants were harvested, ground in liquid N_2, and incubated at 4°C for 3 h with lysis buffer provided in the μMACS HA Isolation Kit (Miltenyl Biotec), containing Protease Inhibitor Cocktail (Sigma-Aldrich). Co-IP was performed using anti-HA magnetic beads from the μMACS HA Isolation Kit (Miltenyl Biotec) and incubating the cell lysis with beads at 4°C for 2 h. LC-MS/MS analysis was performed at the Genome Center of the University of California-Davis, as described previously (Shipman-Roston et al., 2010). Scaffold (version Scaffold 3; www.proteomesoftware.com) was used to validate tandem mass spectrometry-based peptide and protein identification. Peptide identifications were accepted if they could be established at >80.0% probability. Protein identifications were accepted if they could be established at >95.0% probability and contained at least three identified peptides.

For immunoprecipitation of the PsbO protein, seedlings of Col-0, transgenic plant *DEX-AtCV-HA-3*, and *DEX-AtCVΔC-HA* were treated with DEX by the above-mentioned procedures. Cell lysates were incubated with an anti-PsbO antibody coupled to magnetic Dynabeads Protein A (Life Technologies) for 2 h at 4°C. Immunoprecipitated samples were checked by immunoblotting with anti-PsbO and anti-HA antibody, respectively.

BiFC

The four vectors *pDEST-^{GW}VYNE*, *pDEST-VYNE(R)^{GW}*, *pDEST-^{GW}SCYCE*, and *pDEST-SCYCE(R)^{GW}* from the Gateway-based BiFC vector systems (Gehl et al., 2009) were employed to fuse *AtCV*, *PsbO1*, and *SGR1* (At4G22920) with the N terminus of yellow fluorescent protein Venus ($Venus^N$) or the C terminus of super cyan fluorescent protein ($SCFP^C$) to obtain the constructs *AtCV-SCFP^C*, *Venus^N-AtCV*, *PsbO1-Venus^N*, *SCFP^C-PsbO1*, *SGR1-Venus^N*, and *AtCVΔC-SCFP^C*. All the

constructs were introduced into *Agrobacterium tumefaciens* GV3101. Transient expression was performed in cotyledons of Col-0 young seedlings as described previously (Marion et al., 2008).

GUS Staining and Chlorophyll Measurement

For GUS staining, whole seedlings were submerged in standard X-GlcA solution (50 mM sodium phosphate buffer, pH 7.0, 10 mM EDTA, 0.1% Triton X-100, and 0.5 mg/mL X-GlcA) and vacuum infiltrated for 5 min followed by incubation at 37°C for 16 h to develop blue color as described previously (Jefferson et al., 1987).

For chlorophyll measurements, the leaves were weighed and ground in liquid N_2. Chlorophyll was extracted in 80% acetone, and the absorbance at 663 and 645 nm was measured using spectrophotometry (DU-640; Beckman Coulter). Total chlorophyll contents were calculated as described elsewhere (Porra, 2002).

Accession Numbers

Sequence data from this article can be found in the GenBank/EMBL database or the Arabidopsis Genome Initiative database under the following accession numbers: AtCV (AT2G25625), VAMP711 (AT4G32150), PsaB (ATCG00340), Lhcb2 (AT2G05070), PsbA/D1 (ATCG00020), PsbO1 (AT5G66570), PsbO2 (AT3G50820), GS1/GLN1 (AT5G37600), GS2/GLN2 (AT5G35630), SGR1/NYE1 (AT4G22920), CYP20-2 (AT5G13120), FtsH1 (AT1G50250), and Tic20-II (AT2G47840).

Supplemental Data

The following materials are available in the online version of this article.

Supplemental Figure 1. The Dynamics of CCV Localization.

Supplemental Figure 2. Alignment of CV Homologous Genes in the Plant Kingdom.

Supplemental Figure 3. Immunolabeling TEM of CV-GFP in DEX-CV-GFP and Col-0.

Supplemental Figure 4. Detection of CV-HA and PsbO1 by Double Immunolabeling TEM Analysis.

Supplemental Figure 5. CCVs Contain Tic20-II.

Supplemental Figure 6. Autophagy Is Not Involved in Formation and Trafficking of CCVs.

Supplemental Figure 7. CCVs Do Not Overlap with SAVs.

Supplemental Figure 8. CV Overexpression Enhanced Salt Stress-Induced Chloroplast Degradation.

Supplemental Figure 9. Silencing CV Increased Chloroplast Stability.

Supplemental Figure 10. Silencing CV Increased Drought Tolerance.

Supplemental Figure 11. CCVs Contain Thylakoid Proteins CYP20-2 and FtsH1 but Not Plastoglobule Protein.

Supplemental Figure 12. A Proposed Model of CV-Mediated Chloroplast Degradation.

Supplemental Table 1. Proteins Interacting with CV as Identified by Coimmunoprecipitation and Mass Spectrometry.

Supplemental Table 2. Primers Designed for This Study.

ACKNOWLEDGMENTS

We thank Maureen Hanson (Cornell University), Kohki Yoshimoto (Institute Jean-Pierre Bourgin), Richard Vierstra (University of Wisconsin-Madison), and Felix Kessler (Université de Neuchâtel) for providing CT-DsRed, *atg5-1*, GFP-ATG8a, and PGL34-YFP, respectively. This research was supported by the Will W. Lester Endowment of the University of California.

AUTHOR CONTRIBUTIONS

Experiments were designed by S.W. and E.B. S.W. performed most of the experiments. S.W. and E.B. analyzed the data and wrote the article.

Received October 14, 2014; revised November 14, 2014; accepted December 7, 2014; published December 23, 2014.

REFERENCES

Adam, Z., Frottin, F., Espagne, C., Meinnel, T., and Giglione, C. (2011). Interplay between N-terminal methionine excision and FtsH protease is essential for normal chloroplast development and function in *Arabidopsis*. Plant Cell **23:** 3745–3760.

Bassham, D.C. (2009). Function and regulation of macroautophagy in plants. Biochim. Biophys. Acta **1793:** 1397–1403.

Bernhard, W.R., and Matile, P. (1994). Differential expression of glutamine synthetase genes during the senescence of *Arabidopsis thaliana* rosette leaves. Plant Sci. **98:** 7–14.

Carrión, C.A., Costa, M.L., Martínez, D.E., Mohr, C., Humbeck, K., and Guiamet, J.J. (2013). In vivo inhibition of cysteine proteases provides evidence for the involvement of 'senescence-associated vacuoles' in chloroplast protein degradation during dark-induced senescence of tobacco leaves. J. Exp. Bot. **64:** 4967–4980.

Clough, S.J., and Bent, A.F. (1998). Floral dip: A simplified method for Agrobacterium-mediated transformation of *Arabidopsis thaliana*. Plant J. **16:** 735–743.

Dettmer, J., Hong-Hermesdorf, A., Stierhof, Y.D., and Schumacher, K. (2006). Vacuolar H^+-ATPase activity is required for endocytic and secretory trafficking in *Arabidopsis*. Plant Cell **18:** 715–730.

Earley, K.W., Haag, J.R., Pontes, O., Opper, K., Juehne, T., Song, K., and Pikaard, C.S. (2006). Gateway-compatible vectors for plant functional genomics and proteomics. Plant J. **45:** 616–629.

Foresti, O., Gershlick, D.C., Bottanelli, F., Hummel, E., Hawes, C., and Denecke, J. (2010). A recycling-defective vacuolar sorting receptor reveals an intermediate compartment situated between prevacuoles and vacuoles in tobacco. Plant Cell **22:** 3992–4008.

Gan, S., and Amasino, R.M. (1995). Inhibition of leaf senescence by autoregulated production of cytokinin. Science **270:** 1986–1988.

Gehl, C., Waadt, R., Kudla, J., Mendel, R.R., and Hänsch, R. (2009). New GATEWAY vectors for high throughput analyses of protein-protein interactions by bimolecular fluorescence complementation. Mol. Plant **2:** 1051–1058.

Hanson, M.R., and Sattarzadeh, A. (2008). Dynamic morphology of plastids and stromules in angiosperm plants. Plant Cell Environ. **31:** 646–657.

Henmi, T., Yamasaki, H., Sakuma, S., Tomokawa, Y., Tamura, N., Shen, J.R., and Yamamoto, Y. (2003). Dynamic interaction between the D1 protein, CP43 and OEC33 at the lumenal side of photosystem II in spinach chloroplasts: Evidence from light-induced cross-linking of the proteins in the donor-side photoinhibition. Plant Cell Physiol. **44:** 451–456.

Hörtensteiner, S. (2006). Chlorophyll degradation during senescence. Annu. Rev. Plant Biol. **57:** 55–77.

Hörtensteiner, S. (2009). Stay-green regulates chlorophyll and chlorophyll-binding protein degradation during senescence. Trends Plant Sci. **14:** 155–162.

Hoshida, H., Tanaka, Y., Hibino, T., Hayashi, Y., Tanaka, A., Takabe, T., and Takabe, T. (2000). Enhanced tolerance to salt stress in transgenic rice that overexpresses chloroplast glutamine synthetase. Plant Mol. Biol. **43:** 103–111.

Ishida, H., and Wada, S. (2009). Autophagy of whole and partial chloroplasts in individually darkened leaves: A unique system in plants? Autophagy **5:** 736–737.

Ishida, H., and Yoshimoto, K. (2008). Chloroplasts are partially mobilized to the vacuole by autophagy. Autophagy **4:** 961–962.

Ishida, H., Yoshimoto, K., Izumi, M., Reisen, D., Yano, Y., Makino, A., Ohsumi, Y., Hanson, M.R., and Mae, T. (2008). Mobilization of Rubisco and stroma-localized fluorescent proteins of chloroplasts to the vacuole by an ATG gene-dependent autophagic process. Plant Physiol. **148:** 142–155.

Izumi, M., and Ishida, H. (2011). The changes of leaf carbohydrate contents as a regulator of autophagic degradation of chloroplasts via Rubisco-containing bodies during leaf senescence. Plant Signal. Behav. **6:** 685–687.

Izumi, M., Wada, S., Makino, A., and Ishida, H. (2010). The autophagic degradation of chloroplasts via Rubisco-containing bodies is specifically linked to leaf carbon status but not nitrogen status in Arabidopsis. Plant Physiol. **154:** 1196–1209.

Jang, C., Seo, E.Y., Nam, J., Bae, H., Gim, Y.G., Kim, H.G., Cho, I.S., Lee, Z.W., Bauchan, G.R., Hammond, J., and Lim, H.S. (2013). Insights into *Alternanthera mosaic virus* TGB3 functions: Interactions with *Nicotiana benthamiana* PsbO correlate with chloroplast vesiculation and veinal necrosis caused by TGB3 over-expression. Front. Plant Sci. **4:** 5.

Jefferson, R.A., Kavanagh, T.A., and Bevan, M.W. (1987). GUS fusions: Beta-glucuronidase as a sensitive and versatile gene fusion marker in higher plants. EMBO J. **6:** 3901–3907.

Jiang, H., Li, M., Liang, N., Yan, H., Wei, Y., Xu, X., Liu, J., Xu, Z., Chen, F., and Wu, G. (2007). Molecular cloning and function analysis of the stay green gene in rice. Plant J. **52:** 197–209.

Kapri-Pardes, E., Naveh, L., and Adam, Z. (2007). The thylakoid lumen protease Deg1 is involved in the repair of photosystem II from photoinhibition in *Arabidopsis*. Plant Cell **19:** 1039–1047.

Levitt, J. (1972). Responses of Plants to Environmental Stresses. (New York: Academic Press).

Lim, P.O., Kim, H.J., and Nam, H.G. (2007). Leaf senescence. Annu. Rev. Plant Biol. **58:** 115–136.

Lindahl, M., Spetea, C., Hundal, T., Oppenheim, A.B., Adam, Z., and Andersson, B. (2000). The thylakoid FtsH protease plays a role in the light-induced turnover of the photosystem II D1 protein. Plant Cell **12:** 419–431.

Liu, J., Wu, Y.H., Yan, J.J., Liu, Y.D., and Shen, F.F. (2008). Protein degradation and nitrogen remobilization during leaf senescence. J. Plant Biol. **51:** 11–19.

Liu, Y., and Bassham, D.C. (2012). Autophagy: Pathways for self-eating in plant cells. Annu. Rev. Plant Biol. **63:** 215–237.

Livak, K.J., and Schmittgen, T.D. (2001). Analysis of relative gene expression data using real-time quantitative PCR and the 2(-Delta Delta C(T)) method. Methods **25:** 402–408.

Ludlow, M. (1989). Strategies in Response to Water Stress. (The Hague: The Netherlands: SPB Academic Press).

Lundin, B., Hansson, M., Schoefs, B., Vener, A.V., and Spetea, C. (2007). The Arabidopsis PsbO2 protein regulates dephosphorylation and turnover of the photosystem II reaction centre D1 protein. Plant J. **49:** 528–539.

Machettira, A.B., Gross, L.E., Sommer, M.S., Weis, B.L., Englich, G., Tripp, J., and Schleiff, E. (2011). The localization of Tic20 proteins in *Arabidopsis thaliana* is not restricted to the inner envelope membrane of chloroplasts. Plant Mol. Biol. **77:** 381–390.

Makino, A., and Osmond, B. (1991). Effects of nitrogen nutrition on nitrogen partitioning between chloroplasts and mitochondria in pea and wheat. Plant Physiol. **96:** 355–362.

Marion, J., Bach, L., Bellec, Y., Meyer, C., Gissot, L., and Faure, J.D. (2008). Systematic analysis of protein subcellular localization and interaction using high-throughput transient transformation of Arabidopsis seedlings. Plant J. **56:** 169–179.

Martínez, D.E., Costa, M.L., Gomez, F.M., Otegui, M.S., and Guiamet, J.J. (2008a). 'Senescence-associated vacuoles' are involved in the degradation of chloroplast proteins in tobacco leaves. Plant J. **56:** 196–206.

Martínez, D.E., Costa, M.L., and Guiamet, J.J. (2008b). Senescence-associated degradation of chloroplast proteins inside and outside the organelle. Plant Biol. (Stuttg.) **10** (suppl. 1): 15–22.

Mittler, R., and Blumwald, E. (2010). Genetic engineering for modern agriculture: Challenges and perspectives. Annu. Rev. Plant Biol. **61:** 443–462.

Ohsumi, Y. (2001). Molecular dissection of autophagy: Two ubiquitin-like systems. Nat. Rev. Mol. Cell Biol. **2:** 211–216.

Otegui, M.S., Noh, Y.S., Martínez, D.E., Vila Petroff, M.G., Staehelin, L.A., Amasino, R.M., and Guiamet, J.J. (2005). Senescence-associated vacuoles with intense proteolytic activity develop in leaves of Arabidopsis and soybean. Plant J. **41:** 831–844.

Park, S.Y., et al. (2007). The senescence-induced staygreen protein regulates chlorophyll degradation. Plant Cell **19:** 1649–1664.

Peleg, Z., Reguera, M., Tumimbang, E., Walia, H., and Blumwald, E. (2011). Cytokinin-mediated source/sink modifications improve drought tolerance and increase grain yield in rice under water-stress. Plant Biotechnol. J. **9:** 747–758.

Porra, R.J. (2002). The chequered history of the development and use of simultaneous equations for the accurate determination of chlorophylls a and b. Photosynth. Res. **73:** 149–156.

Reguera, M., Peleg, Z., Abdel-Tawab, Y.M., Tumimbang, E.B., Delatorre, C.A., and Blumwald, E. (2013). Stress-induced cytokinin synthesis increases drought tolerance through the coordinated regulation of carbon and nitrogen assimilation in rice. Plant Physiol. **163:** 1609–1622.

Ren, G., An, K., Liao, Y., Zhou, X., Cao, Y., Zhao, H., Ge, X., and Kuai, B. (2007). Identification of a novel chloroplast protein AtNYE1 regulating chlorophyll degradation during leaf senescence in Arabidopsis. Plant Physiol. **144:** 1429–1441.

Reumann, S., Voitsekhovskaja, O., and Lillo, C. (2010). From signal transduction to autophagy of plant cell organelles: Lessons from yeast and mammals and plant-specific features. Protoplasma **247:** 233–256.

Rivero, R.M., Gimeno, J., Van Deynze, A., Walia, H., and Blumwald, E. (2010). Enhanced cytokinin synthesis in tobacco plants expressing PSARK:IPT prevents the degradation of photosynthetic protein complexes during drought. Plant Cell Physiol. **51:** 1929–1941.

Rivero, R.M., Kojima, M., Gepstein, A., Sakakibara, H., Mittler, R., Gepstein, S., and Blumwald, E. (2007). Delayed leaf senescence induces extreme drought tolerance in a flowering plant. Proc. Natl. Acad. Sci. USA **104:** 19631–19636.

Rivero, R.M., Shulaev, V., and Blumwald, E. (2009). Cytokinin-dependent photorespiration and the protection of photosynthesis during water deficit. Plant Physiol. **150:** 1530–1540.

Sakuraba, Y., Schelbert, S., Park, S.Y., Han, S.H., Lee, B.D., Andrès, C.B., Kessler, F., Hörtensteiner, S., and Paek, N.C.

(2012). STAY-GREEN and chlorophyll catabolic enzymes interact at light-harvesting complex II for chlorophyll detoxification during leaf senescence in *Arabidopsis*. Plant Cell **24:** 507–518.

Schwab, R., Ossowski, S., Riester, M., Warthmann, N., and Weigel, D. (2006). Highly specific gene silencing by artificial microRNAs in *Arabidopsis*. Plant Cell **18:** 1121–1133.

Shen, G., Adam, Z., and Zhang, H. (2007). The E3 ligase AtCHIP ubiquitylates FtsH1, a component of the chloroplast FtsH protease, and affects protein degradation in chloroplasts. Plant J. **52:** 309–321.

Shipman, R.L., and Inoue, K. (2009). Suborganellar localization of plastidic type I signal peptidase 1 depends on chloroplast development. FEBS Lett. **583:** 938–942.

Shipman-Roston, R.L., Ruppel, N.J., Damoc, C., Phinney, B.S., and Inoue, K. (2010). The significance of protein maturation by plastidic type I signal peptidase 1 for thylakoid development in Arabidopsis chloroplasts. Plant Physiol. **152:** 1297–1308.

Sirpiö, S., Holmström, M., Battchikova, N., and Aro, E.M. (2009). AtCYP20-2 is an auxiliary protein of the chloroplast NAD(P)H dehydrogenase complex. FEBS Lett. **583:** 2355–2358.

Smaczniak, C., Li, N., Boeren, S., America, T., van Dongen, W., Goerdayal, S.S., de Vries, S., Angenent, G.C., and Kaufmann, K. (2012). Proteomics-based identification of low-abundance signaling and regulatory protein complexes in native plant tissues. Nat. Protoc. **7:** 2144–2158.

Tambussi, E.A., Bartoli, C.G., Beltrano, J., Guiamet, J.J., and Araus, J.L. (2000). Oxidative damage to thylakoid proteins in water-stressed leaves of wheat (*Triticum aestivum*). Physiol. Plant. **108:** 398–404.

Thompson, A.R., Doelling, J.H., Suttangkakul, A., and Vierstra, R.D. (2005). Autophagic nutrient recycling in Arabidopsis directed by the ATG8 and ATG12 conjugation pathways. Plant Physiol. **138:** 2097–2110.

Tian, F., Gong, J., Zhang, J., Zhang, M., Wang, G., Li, A., and Wang, W. (2013). Enhanced stability of thylakoid membrane proteins and antioxidant competence contribute to drought stress resistance in the tasg1 wheat stay-green mutant. J. Exp. Bot. **64:** 1509–1520.

Uemura, T., Ueda, T., Ohniwa, R.L., Nakano, A., Takeyasu, K., and Sato, M.H. (2004). Systematic analysis of SNARE molecules in Arabidopsis: Dissection of the post-Golgi network in plant cells. Cell Struct. Funct. **29:** 49–65.

Vidi, P.A., Kessler, F., and Bréhélin, C. (2007). Plastoglobules: A new address for targeting recombinant proteins in the chloroplast. BMC Biotechnol. **7:** 4.

Vinatzer, B.A., Teitzel, G.M., Lee, M.W., Jelenska, J., Hotton, S., Fairfax, K., Jenrette, J., and Greenberg, J.T. (2006). The type III effector repertoire of *Pseudomonas syringae* pv. *syringae* B728a and its role in survival and disease on host and non-host plants. Mol. Microbiol. **62:** 26–44.

Voss, I., Sunil, B., Scheibe, R., and Raghavendra, A.S. (2013). Emerging concept for the role of photorespiration as an important part of abiotic stress response. Plant Biol. (Stuttg.) **15:** 713–722.

Wada, S., Ishida, H., Izumi, M., Yoshimoto, K., Ohsumi, Y., Mae, T., and Makino, A. (2009). Autophagy plays a role in chloroplast degradation during senescence in individually darkened leaves. Plant Physiol. **149:** 885–893.

Wang, S., Kurepa, J., Hashimoto, T., and Smalle, J.A. (2011). Salt stress-induced disassembly of *Arabidopsis* cortical microtubule arrays involves 26S proteasome-dependent degradation of SPIRAL1. Plant Cell **23:** 3412–3427.

Wang, Y., Yu, B., Zhao, J., Guo, J., Li, Y., Han, S., Huang, L., Du, Y., Hong, Y., Tang, D., and Liu, Y. (2013). Autophagy contributes to leaf starch degradation. Plant Cell **25:** 1383–1399.

Winter, D., Vinegar, B., Nahal, H., Ammar, R., Wilson, G.V., and Provart, N.J. (2007). An "Electronic Fluorescent Pictograph" browser for exploring and analyzing large-scale biological data sets. PLoS ONE **2:** e718.

Yamamoto, Y. (2001). Quality control of photosystem II. Plant Cell Physiol. **42:** 121–128.

Yamamoto, Y., Aminaka, R., Yoshioka, M., Khatoon, M., Komayama, K., Takenaka, D., Yamashita, A., Nijo, N., Inagawa, K., Morita, N., Sasaki, T., and Yamamoto, Y. (2008). Quality control of photosystem II: Impact of light and heat stresses. Photosynth. Res. **98:** 589–608.

Yi, X., McChargue, M., Laborde, S., Frankel, L.K., and Bricker, T.M. (2005). The manganese-stabilizing protein is required for photosystem II assembly/stability and photoautotrophy in higher plants. J. Biol. Chem. **280:** 16170–16174.

Zaltsman, A., Ori, N., and Adam, Z. (2005). Two types of FtsH protease subunits are required for chloroplast biogenesis and photosystem II repair in *Arabidopsis*. Plant Cell **17:** 2782–2790.